Journal of Cleaner Production 233 (2019) 468–481

Contents lists available at ScienceDirect

Journal of Cleaner Production

journal homepage: www.elsevier.com/locate/jclepro

Assessing the potential of soil carbonation and enhanced weathering through Life Cycle Assessment: A case study for Sao Paulo State, Brazil

David Lefebvre [a, *], Pietro Goglio [a, b], Adrian Williams [a], David A.C. Manning [c], Antonio Carlos de Azevedo [d], Magda Bergmann [e], Jeroen Meersmans [a], Pete Smith [f]

[a] School of Water, Energy and Environment, Cranfield University, College Road, Bedford, MK43 0AL, UK
[b] Wageningen Economic Research, Wageningen University & Research, Leeuwenborch, Hollandsweg 1, 6706KN, Wageningen, the Netherlands
[c] School of Natural and Environmental Sciences, Newcastle University, Newcastle Upon Tyne NE1 7RU, UK
[d] USP/ESALQ/LSO, Av. Padua Dias, 11, 13415900, Piracicaba, SP, Brazil
[e] Geological Survey of Brazil (CPRM), Rua Banco da Provincia 105, Porto Alegre, CEP, 90840-030, Rio Grande do Sul, Brazil
[f] Institute of Biological and Environmental Sciences, University of Aberdeen, 23 St Machar Drive, Aberdeen AB24 3UU, UK

ARTICLE INFO

Article history:
Received 17 January 2019
Received in revised form
10 June 2019
Accepted 10 June 2019
Available online 11 June 2019

Keywords:
Life cycle assessment
LCA
Enhanced weathering
Carbonation
NET
Sao paulo

ABSTRACT

Enhanced silicate rock weathering for long-term carbon dioxide sequestration has considerable potential, but depends on the availability of suitable rocks coupled with proximity to suitable locations for field application. In this paper, we investigate the established mining industry that extracts basaltic rocks for construction from the Paraná Basin, Sao Paulo State, Brazil. Through a Life Cycle Assessment, we determine the balance of carbon dioxide emissions involved in the use of this material, the relative contribution of soil carbonation and enhanced weathering, and the potential carbon dioxide removal of Sao Paulo agricultural land through enhanced weathering of basalt rock.

Our results show that enhanced weathering and carbonation respectively emit around 75 and 135 kg carbon dioxide equivalent per tonne of carbon dioxide equivalent removed (considering a quarry to field distance of 65 km). We underline transportation as the principal process negatively affecting the practice and uncover a limiting road travel distance from the quarry to the field of 540 ± 65 km for carbonation and 990 ± 116 km for enhanced weathering, above which the emissions offset the potential capture. Regarding Sao Paulo State, the application of crushed basalt at 1 t/ha to all of the State's 12 million hectares of agricultural land could capture around 1.3 to 2.4 Mt carbon dioxide equivalent through carbonation and enhanced weathering, respectively.

This study suggests a lower sequestration estimate than previous studies and emphasizes the need to consider all process stages through a Life Cycle Assessment methodology, to provide more reliable estimates of the sequestration potential of greenhouse gas removal technologies.

1. Introduction

Scientists agree that, by 2100, the annual extraction of an average of 3.3 Gt of carbon equivalent per year (>12 Gt carbon dioxide equivalent [CO_{2eq}] per year) from the atmosphere will be necessary to limit the increase in global average temperature to 2 °C relative to pre-industrial levels (Fuss et al., 2014; Smith et al., 2016; Williamson, 2016). To mitigate this, it is not only necessary to prevent greenhouse gas (GHG) emissions, but also to remove GHG from the atmosphere. A greenhouse gas removal technology (GGRT) or negative emission technology is one capable of removing GHG from the atmosphere (EASAC, 2018; Fuss et al., 2018; Williamson, 2016; Williamson and Bodle, 2016).

Enhanced weathering (EW) has received increasing interest in the past few years (Martin, 2017; Renforth et al., 2011); its global potential has been addressed by Beerling et al. (2018). It is defined as the *"process by which CO_2 is sequestered from the atmosphere through the dissolution of silicate minerals on the land surface"* (Renforth, 2012) and is regarded as a potential GGRT. Similarly, carbonation is a process where the formation of carbonate minerals in soils is promoted artificially, mimicking natural pedogenic carbonate formation to produce a measurable permanent sink for atmospheric CO_2 (Kolosz et al., 2019; Manning et al., 2013;

* Corresponding author.
E-mail address: D.Lefebvre@cranfield.ac.uk (D. Lefebvre).

https://doi.org/10.1016/j.jclepro.2019.06.099

Washbourne et al., 2015).

Weathering of silicate rock has played a significant role over geological time in the regulation of Earth's climate (Berner and Kothavala, 2001). However, due to the average slow rate of natural rock weathering, its effect on a human time scale is too slow to compensate for artificial changes in atmospheric composition (Hartmann et al., 2009; Taylor et al., 2017). To accelerate the process, EW and carbonation rely on the comminution of the rock, increasing its reactive surface, hence promoting its dissolution and thus its CO_2 capture rate (Taylor et al., 2017).

Although studied, the magnitude of worldwide carbon capture potential through EW varies depending on the application area considered, type of rock used, and application rate (Beerling et al., 2018; Moosdorf et al., 2014). Life Cycle Assessments (LCA) of the CO_2 sequestration potential of silicate rock exist, however the process studied involves direct fluxes of CO_2 in a reactor at high temperature and pressure (Khoo et al., 2011; Nduagu et al., 2012), which clearly differs from the natural dissolution process under ambient Earth-surface conditions studied here. No study has yet assessed in detail the environmental costs and impacts linked to the natural dissolution processes of this soil-based GGRT. Sao Paulo State (Brazil) was selected as a case study, because of a combination of unique factors: the geographical colocation of the Paraná flood basalts (Hartmann and Moosdorf, 2012) with large scale agricultural production that is amenable to application of rock dust within the Brazilian regulatory system for remineralizers (Manning and Theodoro, 2018). Our findings can be applied to other regions where suitable rocks are spatially associated with appropriate land management (Beerling et al., 2018).

This study i) assesses the environmental impacts of the practice using basalt rock in Sao Paulo state conditions including the emissions associated with the rock extraction, comminution, transport and application through a Life Cycle Assessment approach; ii) estimates the contribution of the different processes involved with soil carbonation and enhanced weathering and iii) assesses the potential CO_2 removal of Sao Paulo agricultural land through soil carbonation and weathering of basalt rock. A large number of active mining operations occur within the Paraná flood basalts. These supply aggregate for construction; in providing low-cost products using existing technology, they represent a well-established mining sector that is expected to grow with increasing urbanisation.

2. Methodology

2.1. Chemical aspects

The process of rock weathering involves a series of chemical reactions. First, the hydration of CO_2 (Equation (1)) forms carbonic acid (Martin, 2017).

Equation (1): CO_2 hydration

$$CO_2 + H_2O \leftrightharpoons H_2CO_3 \quad (1)$$

This weak acid breaks down silicate rock, which releases base cations (e.g. Ca^{2+}, Mg^{2+}) and bicarbonate and carbonate ions (Beerling, 2017) in proportion depending on pH. The weathering of silicate minerals is commonly represented using the calcium silicate mineral wollastonite ($CaSiO_3$), and releases bicarbonate ions (Equation (2)).

Equation (2): Weathering of wollastonite

$$CaSiO_3 + 2H_2CO_3 \rightarrow Ca^{2+} + 2HCO_3^- + SiO_2 + H_2O \quad (2)$$

Following Equation (2), when the dissolved bicarbonate ions are then transferred to the ocean and contribute to its alkalinity, two moles of CO_2 are captured per mole of calcium (content depending on the rock). This path will be herein referred to as enhanced weathering (EW) (Equation (3)).

Equation (3): Enhanced Weathering (EW) (Wollastonite)

$$CaSiO_3 + 2CO_2 + 2H_2O \rightarrow Ca^{2+} + 2HCO_{3\,(to\ Ocean)}^- + SiO_2 + H_2O \quad (3)$$

However, when soil conditions are favourable, some of the calcium and magnesium cations can precipitate to form carbonate minerals (Equation (4)), which accounts for half the moles of CO_2 captured during the weathering of the rock. The latter path will be herein referred to as carbonation (Equation (4)).

Equation (4): Carbonate mineral formation (Carbonation)

$$\begin{aligned} &CaSio_3 + 2CO_2 + 2H_2O \rightarrow Ca^{2+} + 2HCO_3^- + SiO_2 + H_2O \\ &\boldsymbol{Ca}^{2+} + 2\boldsymbol{HCO}_3^- \leftrightarrow CaCO_{3(\ in\ soils)} + CO_2 + H_2O \end{aligned} \quad (4)$$

The capture potential of each path (i.e. Carbonation and EW) depends on the type of rock used. Minerals in ultrabasic rocks, such as olivine (Mg_2SiO_4), weather relatively quickly and show a high potential for CO_2 sequestration (Goldich, 1938; O'Connor et al., 2005). However, several studies suggest that the weathering of olivine-bearing rocks could lead to the release of chromium (Cr) and nickel (Ni) into the environment, which if sufficient, suppresses calcium uptake by plants (Renforth et al., 2015; ten Berge et al., 2012) and could be toxic, although they are essential to life in small amounts. Importantly, current mining of olivine-rich rocks is limited to a small number of locations globally.

In addition, basic rocks, such as basalt, occur widely and show great potential for enhanced weathering, despite their lower sequestration potential than olivine (0.3t CO_{2eq}/t for basalt and 0.8t CO_{2eq}/t for olivine in the case of EW) (Beerling et al., 2018; Strefler et al., 2018). Basalt is globally available in large quantities, has a fast weathering rate, and has lower concentrations of Cr and Ni and a higher concentration of phosphorus, thus posing fewer environmental risks through its application (Beerling et al., 2018; Bryan and Ernst, 2008; Kantola et al., 2017). It is widely mined for construction, and used in agriculture for remineralization (Manning and Theodoro, 2018).

2.2. Sequestration potential of brazilian basalt rock

The potential CO_2 capture of basalt rock is calculated using Equation (5) from Renforth (2012).

Equation (5): Sequestration potential

$$R_{CO_2} = \frac{M_{CO_2}}{100}\left(\frac{\%CaO}{M_{CaO}} + \frac{\%MgO}{M_{MgO}}\right) * \omega \quad (5)$$

where R_{CO2} is the sequestration potential in tonne CO_{2eq} per tonne of rock; M_{MgO}, M_{CaO}, and M_{CO2}, as the molecular masses of MgO, CaO and CO_2, respectively; %CaO and %MgO the percent in weight of CaO and MgO in the rock, respectively; and ω, a factor that accounts for the additional sequestration that occurs when the cations are transported to the oceans and remain dissolved.

The potential CO_2 capture through carbonation is calculated using the CaO and MgO content of the rock and assuming the precipitation of the associated cations (i.e. Ca^{2+} and Mg^{2+}) into carbonate minerals (i.e. calcite and magnesite). Since no cations are transferred into the ocean, the value of ω for carbonation is one. Average MgO and CaO contents were computed from 48 measurements of Brazilian basalt (Baggio et al., 2016; Braz Machado et al., 2018; Moraes et al., 2018) and averaged as 4.87 and 9.14% by weight, respectively, leading to a capture potential through

carbonation of 0.125 t CO_{2eq}/t of basalt.

CO_2 capture through enhanced weathering assumes that all the cations, resulting from the dissolution of the rock, remain dissolved and are transferred to the ocean. Only ω changes in Equation (5). According to Kheshgi (1995), when all cations remain dissolved, the value of ω reaches 1.79 which means that 1.79 moles of CO_2 is sequestered per mole of CaO or MgO. Using the value of 1.79 for ω, the potential sequestration through EW reaches 0.225 t CO_{2eq}/t of basalt. A ω value of 1.7 was used in other publications on enhanced weathering (Harvey, 2008; Renforth, 2012). Overall, the widely used sequestration value through EW of 0.3 t CO_2/t of basalt (Beerling et al., 2018; Kantola et al., 2017; Strefler et al., 2018) results from Equation (5) using different average values for CaO and MgO content and a value of 1.7 for ω.

This study considers both the carbonation and EW pathway. Although carbonation is likely after the application of the rock on the field (Manning and Renforth, 2013), EW is expected to happen simultaneously and further dissolution of the calcite and magnesite produced through carbonation may also occur (Landi et al., 2003). Therefore, the sequestration potentials though carbonation and EW presented here represent lower and upper limits, respectively. The actual sequestration value after the application of one tonne of basalt on a field is likely to be between these two limits. The sequestration rate through carbonation or EW depends on the rock weathering rate that varies greatly depending on various factors. Although not studied here, the matter is discussed later.

Fig. 1 provides an overview of the weathering process as well as the two considered paths and their sequestration potentials for Brazilian basalt rock.

2.3. Study area

We selected Sao Paulo (SP) State due to its situation on an area with large basalt deposits (Bryan and Ernst, 2008; Hartmann and Moosdorf, 2012), the resulting occurrence of basalt quarries (DNPM, 2018; Perrotta et al., 2006), and the climatic and soil conditions for rapid rock weathering (Edwards et al., 2017; Meysman and Montserrat, 2017). Further, the practice is already used by farmers in the area as a soil remineralizer.

Fig. 2 shows SP with the locations of basalt quarries, cropland, and grassland inside the state. Concentric buffer zones, centred on the quarries, represent straight-line distances between quarries and agricultural areas. The distance increments were selected arbitrarily. The maximum distance of 250 km was selected because it covers the totality of Sao Paulo's agricultural area.

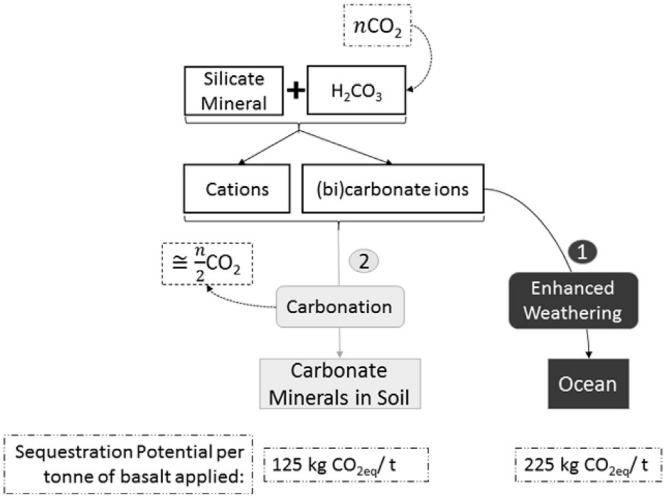

Fig. 1. Overview of the rock weathering process, the two pathways (carbonation and EW) considered in this study and the sequestration potential of Brazilian basalt for each considered path.

The average quarry to field distance of 50 km was calculated by summing the product of each distance increment by the agricultural area it covers, and dividing the result by the total agricultural area of SP.

Data on land use was provided by the "ESA Climate Change Initiative" (UCLouvain, 2017) and the area of cropland and grassland reported is consistent with the Brazilian Institute of Geography and Statistics (IBGE, 2017). The location of the basalt quarries in SP was provided by the "National Geology Program of Brazil" (Perrotta et al., 2006).

2.4. Objectives and system boundary

To assess the environmental impacts of basalt rock application the following processes were considered within the system boundary: the extraction of the material, its transport to the grinding facility, its comminution into particles of <5 mm, its transport from quarries to the fields, and its spreading on the field using agricultural spreaders (Fig. 3). This LCA does not take into account any soil or crop response following the field application. Each process stage is described below.

The functional units (FU) of this LCA are i) per hectare of SP agricultural land amended by < 5 mm basalt particles, and ii) per tonne of CO_{2eq} removed.

Distances from quarry to field are represented nominally in straight lines in our map (Fig. 2). Road tortuosity ratio is a coefficient used to consider the tortuosity of the road network of an area. Multiplying the coefficient by the linear distance between two points gives a more accurate estimate of journey length through the road network.

We found a tortuosity ratio of 1.3 by comparing 30 actual road (randomly selected) and straight-line distances inside the state. We then multiplied every linear distance by this ratio to calculate the transport impacts. The average quarry to field distance of 50 km discussed earlier becomes 65 km once accounting for the road tortuosity of Sao Paulo state.

We considered three basalt application rates: 5, 50, and 20 t/ha. The first application rate is representative of what is currently spread by some farmers in Sao Paulo (according to two local experts) as well as the minimum recommended rate according to two UK rock dust retailers (Ramezanian et al., 2013; REMIN, n.d.). The second application rate of 50 t/ha represents the maximum dose considered in the literature for carbon sequestration purposes (Beerling et al., 2018). The intermediate application rate of 20 t/ha was selected because it has already been used in previous field research in Sao Paulo and corresponds to the recommended application rate according to a UK rock dust retailer (REMIN (Scotland) Ltd, n.d.).

2.5. Software, database & data processing

Most of the activity data regarding quarry processes in our Life Cycle Inventory are based on Rosado et al. (2017). The values used for our analysis are given in Table 1.

Background information was collected using SimaPro 8.3 databases (EcoInvent 3 and USLCI), while SimaPro software was used to compute the Life Cycle Inventory (LCI) and Life Cycle Impact Assessment (LCIA) calculation. We used ArcGIS desktop (ESRI, 2011) to create the map and buffer areas, and Google Earth (Google, 2018) to calculate the tortuosity ratio of Sao Paulo state.

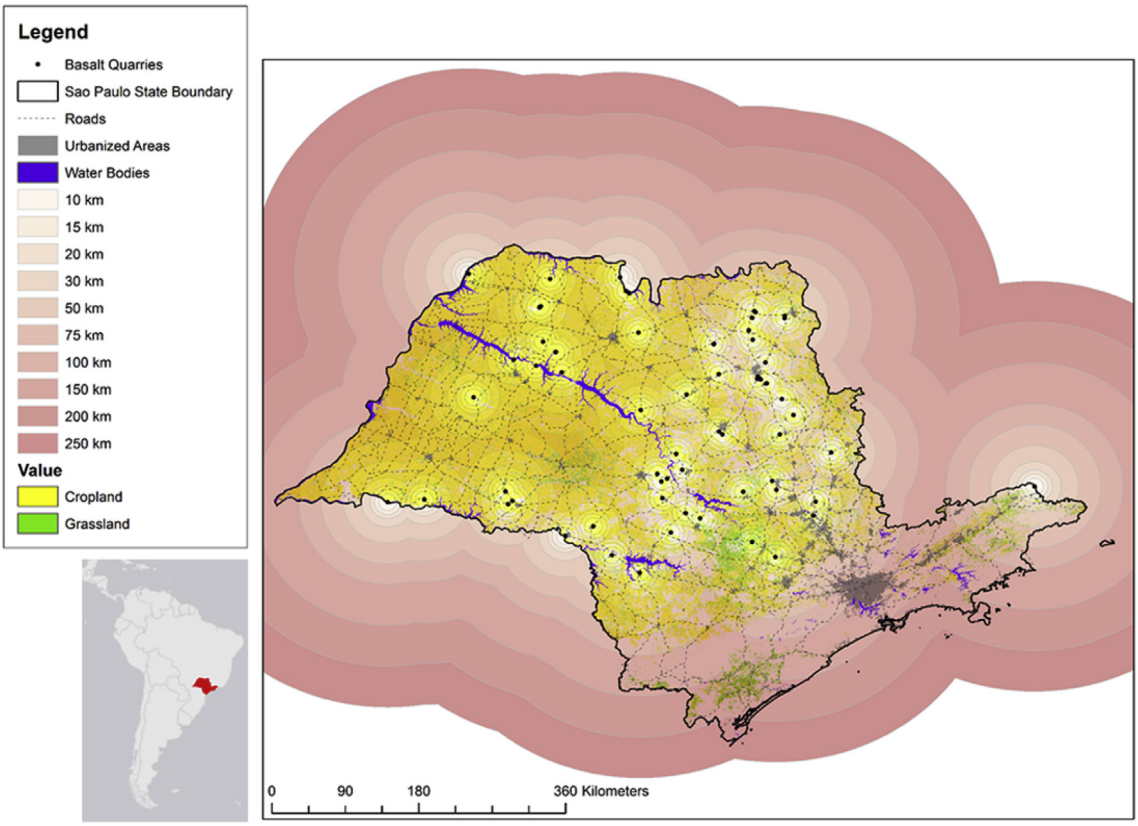

Fig. 2. Sao Paulo state with buffer zones (red shade) around Sao Paulo's basalt quarries overlapping grassland and cropland areas.

2.5.1. Rock extraction

The basalt quarry and production facilities studied here typically have a production capacity of 167 tonnes of aggregate per hour (Rosado et al., 2017). The extraction of the rock starts with drilling to insert explosives (Rosado et al., 2017). The shattered basalt is then loaded in a truck, using a front loader, and transported one km away from the pit, to the processing facility (Rosado et al., 2017).

2.5.2. Rock comminution

For this study, we selected a particle size of 5 mm, corresponding to the high end of what is widely referred to as fine aggregate (Mitchell et al., 2008). In practice, the <5 mm crushed fraction has a wide range of particle size, thus including fine dust. Its production corresponds, in part, to the process of manufacturing construction aggregates, in which all costs are minimised to provide competitive low-cost products in large quantities. Thus, the process inherently minimises energy consumption, and utilises widely used machinery.

The blasted pieces of rock are ground through successive crushers to reach 5 mm. The primary crusher (i.e. jaw crusher) with output particle size of 50 mm is as specified by Rosado et al. (2017). The number and model of additional crushers were selected according to their reduction ratios, feed size acceptance, and crushing rates using the guidelines provided by Metso (2015). Two additional crushers are required, a secondary crusher GP100S and a tertiary cone crusher HP200. The different stages of the crushing process are shown in Fig. 4. All machines are powered by electricity; their energy requirements can be found in Table 2.

2.5.3. Rock transport

After comminution, the ground basalt is loaded in a truck using a front loader and transported to the field. The rock transport is assumed to be carried out only by truck, as it is the main means of transportation in Brazil (Araújo et al., 2013; Wanke and Fleury, 2006).

Sao Paulo state is described as “irregular plains”, with large homogeneous plain areas and a division between the east central and western part of the state by tableland (Manfré et al., 2015). The homogeneity of the land and absence of mountains ensure a reasonably constant fuel consumption throughout the state. Additionally, the majority of the roads in SP are considered in “optimal” or “good condition” (CNT Confederacao National do Transporte, 2017), hence road quality is assumed to have no influence on fuel consumption.

The process used in our study considers the transportation of the material from the quarry to heaps at the edge of field and includes the return of the empty truck to the quarry (Weidema et al., 2013).

2.5.4. Rock spreading

The delivered basalt is then loaded using a front loader into the field spreader, which was assumed to be a conventional lime spreader.

We calculated the diesel consumption for the spreading of the material according to the agricultural machinery consumption from Goglio et al. (2018). We used the average Sao Paulo tractor power from Felipe et al. (2008) and working speed, width and application rate from Brazilian agricultural machinery retailers.

2.6. Impact assessment

We accounted for acidification and abiotic depletion according

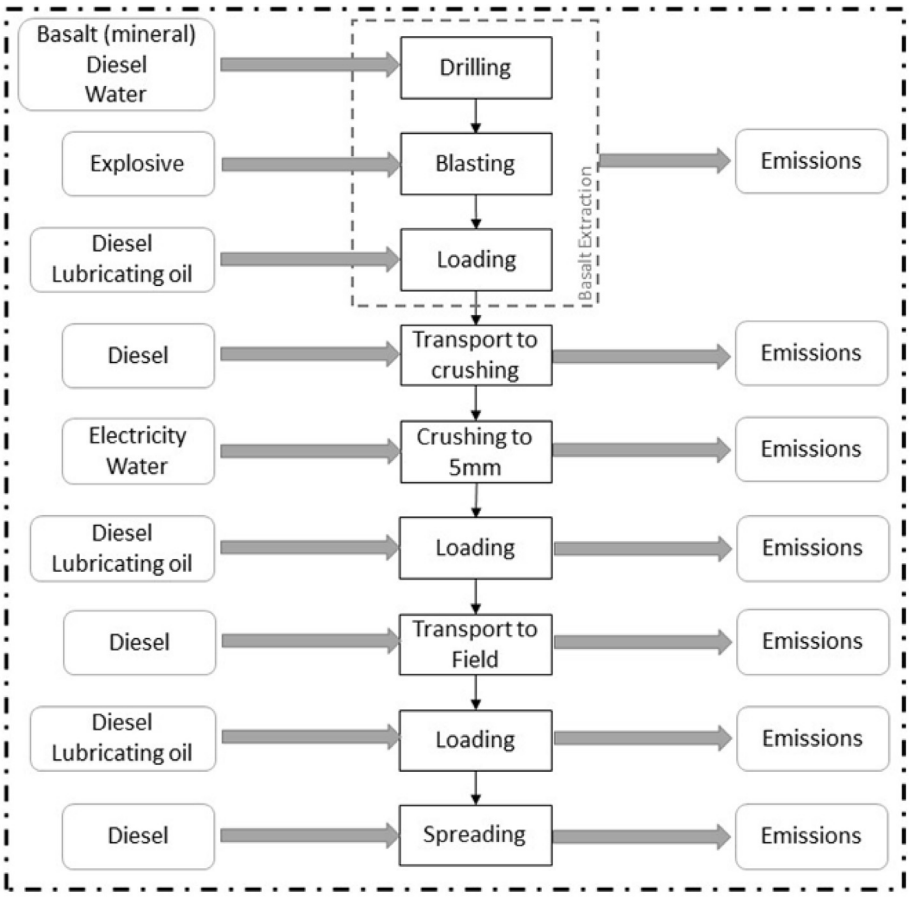

Fig. 3. System boundaries for extraction, comminution, transport and spreading of basalt considered in this study.

to the CML methodology (Guinee et al., 2002), human toxicity, cancer and non-cancer, as well as freshwater ecotoxicity according to the USEtox model (Fantke et al., 2017). Cumulative energy demand (CED) was considered according to the method published by EcoInvent version 2.0 (Frischknecht et al., 2007). GHG balance accounting for the global warming potential (GWP) over a timeframe of 100 years is in accordance with the characterisation factors of the 5th assessment report of the intergovernmental panel on climate change (IPCC, 2014). Units CTUh and CTUe are defined according to Golsteijn (2014). The slope and constant for each linear

Table 1
Database and process used in the LCI of basalt extraction, comminution, transport and spreading.

Process Stage	SimaPro 8.3.0.0 Process	Updates	Unit	Amount [Mg^{-1}]
Basalt Extraction				
Basalt Drilling	Loader operation, large, [a]	Diesel and oil consumption	hour	0.00600
Blasting	Blasting [b]| processing |[c]	Mass of explosive	kg	0.145
Loading Operation				
Front Loader	Loader operation, large, [a]	Diesel and oil consumption	hour	0.00600
Transport to Crushing				
Lorry	Transport, freight, lorry 16–32 metric ton, EURO4 [b] |[c]	/	tkm	1
Crushing to 5 mm				
Electricity	Electricity, medium voltage {BR}| electricity voltage transformation from high to medium voltage |[c] Electricity, medium voltage {BR}| market for |[c]	/	kWh	5.45
Loading Operation				
Front Loader	Loader operation, large, [a]	Diesel and oil consumption	hour	0.00600
Transport to field				
Lorry	Transport, freight, lorry 16–32 metric ton, EURO4 [b] |[c]	/	tkm	65
Loading Operation				
Front Loader	Loader operation, large, [a]	Diesel and oil consumption	hour	0.00600
Spreading on field				
Diesel in Agri Spreader	Diesel, low-sulfur [b] | market for |[c]	/	kg	1.73

[a] Northeast/North Central (NE/NC) region of the US (NE-NC/RNA - USLCI database).
[b] "Rest-of-the-World" geographical consideration (RoW - EcoInvent 3 database).
[c] Allocation default unit process (Alloc Def, U - EcoInvent 3 database).

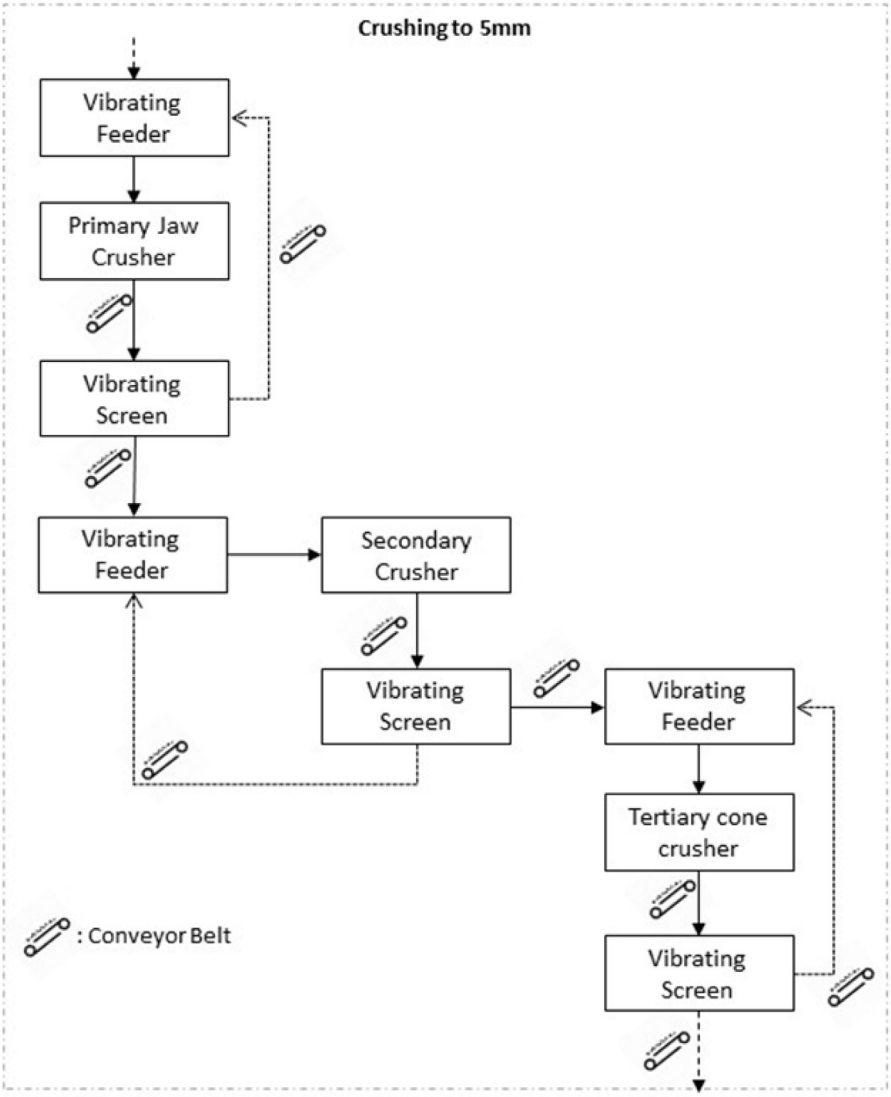

Fig. 4. Crushing process stages considered to reach 5 mm diameter particles of basalt based on Rosado et al. (2017) and Metso (2015).

equation were calculated using Excel and based on the trend line associated with the impact category.

2.7. Estimating Sao Paulo state potential

To approximate the capture potential of SP state, we first calculated the net theoretical sequestration potential of each buffer zone by multiplying the agricultural area of the considered buffer zone by the sequestration potential of EW and carbonation (i.e. 225 kg and 125 kg CO_{2eq}/t of rock applied, respectively). We then subtracted the emissions associated with the setup of the practice for the considered buffer zone. The quarry to field distances used for the calculation of the emissions were the straight line distances to each buffer zone multiplied by the road tortuosity ratio of 1.3. Finally, we summed the net sequestration potential of each buffer zone inside SP.

2.8. Energy for comminution

The energy requirements to reach a 5 mm diameter size particle is based on the machinery recommendation from Metso (2015), and the available data from Rosado et al. (2017). Still according to

Table 2
Energy requirements of crushing process equipment, as metered electricity.

Item	Number of units	Electricity per unit (kWh/t of rock)	Data Origin
Vibrating feeder	3	0.176	Rosado et al. (2017)
Conveyor Belt	9	0.264	Rosado et al. (2017)
Vibrating Screen	3	0.176	Rosado et al. (2017)
Primary Jaw Crusher	1	0.659	Rosado et al. (2017)
Secondary Crusher GP100S	1	0.539	Metso (2015)
Tertiary Cone Crusher HP200	1	0.820	Metso (2015)
Total	**18**	**5.450**	

Metso (2015), the energy needed to specifically grind particles finer than 5 mm is based on Bond's equation:

Equation (5): Bond's Equation

$$W = 10Wi\left(\frac{1}{\sqrt{P_{80}}} - \frac{1}{\sqrt{F_{80}}}\right)$$

With W: Energy [kWh/t]; Wi: Empirical Work Index of the Material [kWh/t]; and P_{80} & F_{80} : Size of particles for which 80% of the product or feed respectively passes through the mesh [μm]

According to this equation, the energy required for grinding increases exponentially as the product maximum particle size gets smaller.

To calculate the energy demand for further grinding from a particle size of 5 mm, we used the work index of basalt for grinding of 17.10 (Kanda and Kotake, 2007; Metso, 2015), and added the energy of three conveyor belts, one vibrating feeder, and one vibrating sieve to account for the additional machinery needed.

2.9. Uncertainty analysis

Uncertainty analysis was conducted using a numerical approach based on Monte Carlo simulations in R software (Core Team, 2018). For each simulation, 10,000 values were randomly selected from each process's distribution. Computation of the uncertainty related to the sequestration potential of basalt included the observed correlation between CaO and MgO contents when randomly selecting values in the distributions. Additional information about the uncertainty analysis can be found in the supplementary material.

3. Results

3.1. Life Cycle Impact Assessment

We calculated the values of each impact category using the average quarry to field distance of 65 km accounting for road tortuosity (Table 3). Results show that the impacts per hectare increase proportionally with the rate of application while the results per tonne of CO_{2eq} removed occur independently of application rate and are inversely proportional to the sequestration potential of the path (EW & carbonation).

Our contribution analysis (Fig. 5) shows the share of each process stage for the impact categories assessed using the average quarry to field distance (i.e. 65 km). The results show that transportation accounts for the majority of the impact categories, ranging from 35% for acidification to 88% for abiotic depletion.

Fig. 6 represents the effect of an increasing quarry to field distance on the GHG balance impact category with a fixed application rate of 5 t/ha. Results show that transportation impact increases as distance increases while crushing, loading, spreading, and blasting process stages remain unchanged, and thus can be considered as "*spatially static*" (Moosdorf et al., 2014).

Fig. 7 illustrates the increase of the GHG emissions associated with the transportation stage as the quarry to field distance increases (grey line). The blue line represents the same trend with the added GHG balance impacts of the spatially static process stages and the orange line, the proportion of transportation within the value of total GHG balance. Fig. 7 shows that the trend is linear and thus that the impact value increases proportionally with the quarry to field distance.

These results show that not only is truck transportation the most impacting process of the practice (when considering the average quarry to field distance) (Fig. 5), but also that the values for each impact category can be readily derived from linear equations because of the proportional trend between quarry to field distance and transportation impact (Fig. 7).

Table 4 gives the slope and constant values for the impact category assessed. Values are shown for the baseline application rate of 1 t/ha.

3.2. CO_{2eq} capture potential of Sao Paulo State

Table 5 shows how the net sequestration potential of Sao Paulo state was calculated for an application rate of 5 t/ha. The column "distance quarry field" represents the concentric buffer zone distances of Fig. 2 updated with the tortuosity ratio of 1.3 discussed in Section 2.4. The "agricultural area covered" column shows the number of hectares included in each of the buffer zone, considering all quarries in SP. The emissions associated with the setup of the practice at the different distance range are reported in the "total GHG balance" column and the values consider the application rate of 5 t/ha of ground basalt on all the hectares within the buffer zone considered. The "net sequestration" columns results from the subtraction of the emission associated with the practice from the potential sequestration (125 and 225 kg CO_{2eq} per tonne of rock applied for carbonation and EW respectively), within a buffer zone, and according to the number of hectares associated. The "loss ratio" represents the part of the sequestration potential that is lost throughout the setup of the practice. The loss ratio increases greatly with the quarry to field distance due to the impact of truck transportation.

Table 6 shows the potential net sequestration of the state for the different rates of application considered (5, 20, 50 t/ha), and compares it with the 2016 emissions of SP state (SEEG, 2016a), Brazil (SEEG, 2016b), and the world (Olivier et al., 2017).

4. Discussion

4.1. GHG removal potential

Several publications have attempted to estimate the sequestration potential of EW (EASAC, 2018). Although some relied on theoretical calculation to assess the energy cost to implement the practice, most provide overestimated sequestration values.

For instance, Kantola et al. (2017) suggest that 1.1 Pg CO_{2eq} could be sequestered by the application of 50 t/ha of basalt on the 70×10^6 ha of the corn belt of North America. However, let us hypothesize that i) the North American production system of 5 mm basalt particles is equivalent to the one represented in this study; ii) that 50% of the material takes the EW path and the other 50% the carbonation path; iii) that all the considered croplands are situated at an average road distance of 65 km from the closest basalt mine (it may be much more than this in agricultural parts of North America); iv) and that the topography and road quality of the area does not affect the emissions of the truck transport. Then, when accounting for the burdens of our optimistic hypothetical system, only 50% (0.55 Pg CO_{2eq}) of the potential postulated by Kantola et al. (2017) can be reached.

The difference between Kantola et al. (2017)'s prediction and ours results from the voluntary omission of the emissions associated with the setup of the practice by Kantola et al. (16.8 kg CO_{2eq}/t of rock in our hypothetical system) and an estimated sequestration potential of basalt of 0.32 t CO_{2eq}/tonne of rock as compared to our average 0.175 t CO_{2eq}/tonne of rock ((225 [EW]+125 [carbonation])/2).

As distance from quarry to field increases, further reduction in the average sequestration potential of basalt is observed and declines to 147 and 125 kg CO_{2eq}/tonne of rock when the quarry to field distance reaches 130 and 260 km of flat, good quality road, respectively.

Table 3
LCIA results for three application rates. Results are shown per hectare and per tonne of CO_{2eq} removed according to the two paths (EW & Carbonation).

Impact Category	Unit	Application Rate [t/ha]	Total [per hectare]	Total Carbonation [per tonne CO_2 removed]	Total EW [per tonne CO_2 removed]
GHG balance	kg CO_2e	5	84.1	135	75.1
		20	337		
		50	842		
CED	MJ	5	1647	2635	1471
		20	6588		
		50	16470		
Abiotic Depletion	kg Sb eq	5	1.74E-04	2.79E-04	1.56E-04
		20	6.97E-04		
		50	1.74E-03		
Acidification	kg SO_2 eq	5	0.618	0.990	0.552
		20	2.47		
		50	6.18		
Freshwater ecotoxicity	CTUe	5	323	517	289
		20	1293		
		50	3233		
Human Toxicity, Cancer	CTUh	5	2.23E-06	3.57E-06	1.99E-06
		20	8.92E-06		
		50	2.23E-05		
Human Toxicity, Non Cancer	CTUh	5	1.81E-05	2.89E-05	1.61E-05
		20	7.23E-05		
		50	1.81E-04		

CTUh: "estimated increase in morbidity (the number of disease cases) in the total human population per unit of mass of the chemicals emitted." (Laura Golsteijn, 2014).
CTUe: "estimated potentially affected fraction of species integrated over time and the volume of the freshwater compartment, per unit of mass of the chemicals emitted." (Laura Golsteijn, 2014).

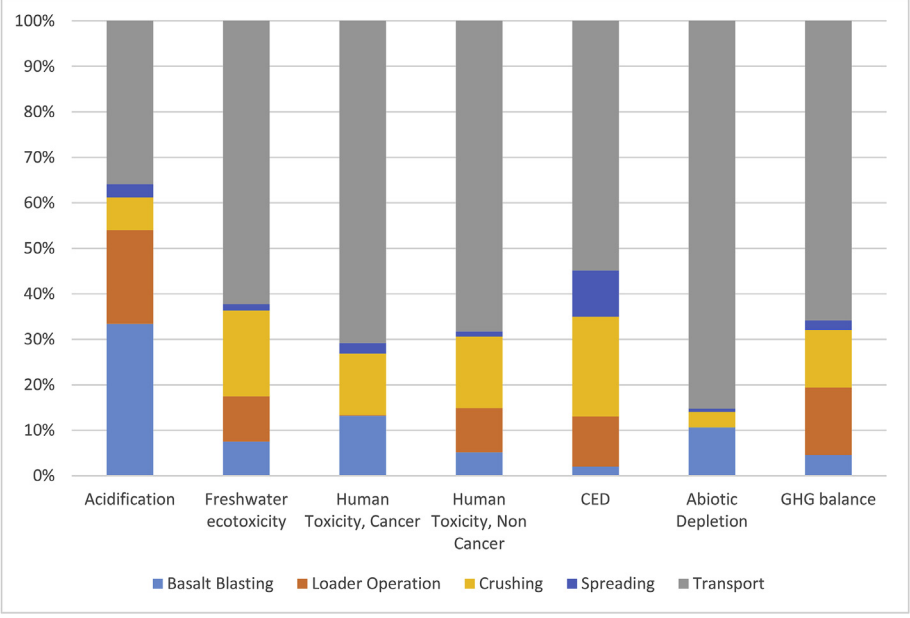

Fig. 5. Impact categories contribution analysis considering the quarry to field distance of 65 km.

4.2. Co-benefits/drawbacks to basalt dust addition

In addition to its carbon capture capacity, studies suggest that the weathering of basalt rock on soils improves crop growth and soil fertility (reviewed by Beerling et al., 2018). According to these studies, the addition of basalt rock dust to soil provides a slow release of nutrients, increases yield and CEC, rebalances soil pH, increases plant resistance to insects, disease, frost and drought, and increases microorganism growth and earthworm activity, among other things (Bergmann et al., 2013; Campe et al., 2015; Gillman et al., 2002; Harley and Gilkes, 2000; Kantola et al., 2017; Leonardos et al., 1998; Manning, 2010; Massey et al., 2007; Melo et al., 2012; Mersi et al., 1991; Nunes et al., 2014; Ramos et al., 2017, 2015; Theodoro and Leonardos, 2006).

From an LCA perspective, the resulting increased biomass, reduced use of fertilizers and pesticides, and the potential removal of the need for lime application (Kantola et al., 2017) (and decrease of linked soil CO_2 emissions (Beerling et al., 2018)) would all contribute to the reduction of the carbon footprint per unit crop output and per ha associated with basalt addition.

The impacts of these benefits are soil, climate and plant specific hence they are impossible to determine in a coarse scale assessment. However, it is reasonable to expect further reductions in the carbon footprint of the overall practice.

Negative impacts related to the addition of basalt, such as possible increased turbidity in drainage to nearby streams or rivers

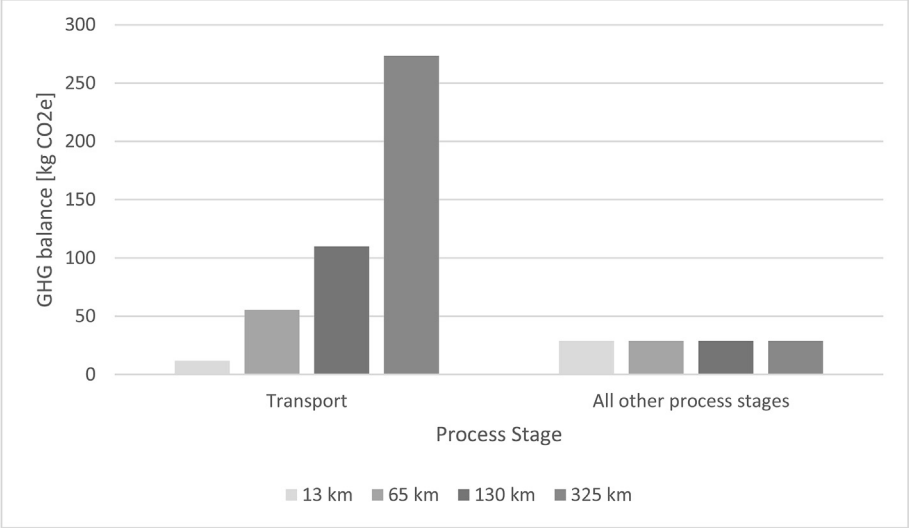

Fig. 6. Effect of an increasing quarry to field distance on the process stages considering GHG balance [kg CO_{2eq}] impact category and an application rate of 5 t/ha.

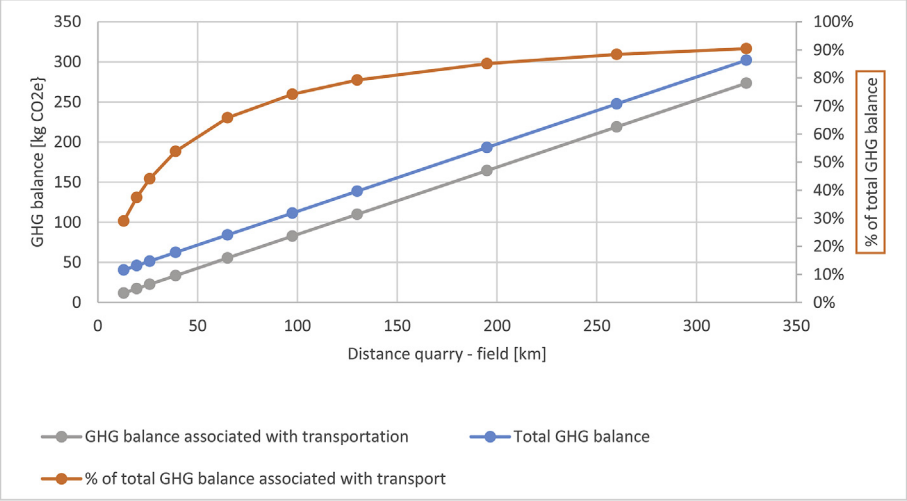

Fig. 7. Share increase of transport linked with increasing quarry to field distance [km] considering total GHG balance impact category and an application rate of 5 t/ha.

Table 4
Slope and constant of each impact category for linear prediction.

Impact Category	Unit	Application Rate [t/ha]	Slope	Constant
GHG balance	kg CO_{2eq}	1	0.218	5.92
CED	MJ	1	3.56	151
Freshwater ecotoxicity	CTUe	1	0.610	25.0
Abiotic Depletion	kg Sb eq	1	5.85E-07	5.60E-06
Acidification	kg SO_2 eq	1	8.74E-04	8.00E-02
Human Toxicity, Cancer	CTUh	1	6.22E-09	1.35E-07
Human Toxicity, Non Cancer	CTUh	1	4.86E-08	1.19E-06

The linear equation $y = mx + b$ with y: the value of the impact category; x: the quarry to field distance in km; m: the slope; and b: the constant.The constant and slope should be multiplied beforehand by the application rate considered.

due to unweathered particles (Edwards et al., 2017; Kohler et al., 2010) may be expected as well; the use of a <5 mm fraction rather than a finely milled (e.g. <100 μm) fraction may mitigate this. The net effects on other categories such as eco or human toxicity impact categories are unclear, but they do not affect net C sequestration.

4.3. Particle size and weathering rate

Several studies promote the use of fine dust particles (10–30 μm diameter) for their rapid carbon sequestration potentials (Beerling et al., 2018; Kohler et al., 2010; Moosdorf et al., 2014). However, although the particulate emissions (PM_{10}) impact category was not assessed in our LCA due to lack of data on the spreading process

Table 5
Emissions and net sequestration in kt CO_{2eq} for the implementation of the practice considering the area included under each buffer zones (with application rate of 5 t/ha).

Distance Quarry - Field [km]	Agricultural Area covered [Million ha]	*Application Rate:* 5 t/ha			Loss Ratio (Carbonation)
		GHG balance[a]	Net sequestration (Carbonation)[a]	Net sequestration (EW)[a]	
13	0.781	31.6	456	843	6.5%
19.5	0.835	38.4	483	897	7.4%
26	0.999	51.3	573	1,067	8.2%
39	2.17	135	1,223	2,298	10.0%
65	3.57	300	1,931	3,698	13.5%
97.5	2.19	244	1,123	2,206	17.8%
130	0.814	113	396	798	22.2%
195	0.222	42.8	95.8	206	30.9%
260	0.102	25.2	38.3	88.7	39.6%
325	0.000376	0.114	0.121	0.307	48.4%
TOTAL	**11.7**		**6.32**	**12.10**	

[a] Emissions and sequestration values for the area covered under the considered buffer zone. In kt CO_{2eq}.

Table 6
Sao Paulo (SP) CO_{2eq} sequestration potential through carbonation and EW as compared with 2016 SP, Brazilian, and global CO_{2eq} emissions. Expressed in Mt CO_{2eq}.

Application Rate	SP net sequestration Potential [Mt CO_{2eq}]		SP Emission 2016	Brazil Emission 2016	World Emission 2016
			159 [Mt CO_{2eq}]	2278 [Mt CO_{2eq}]	46400 [Mt CO_{2eq}]
5 t/ha	Carbonation	6.32	3.98%	0.28%	0.01%
	EW	12.1	7.62%	0.53%	0.03%
20 t/ha	Carbonation	25.3	15.91%	1.11%	0.05%
	EW	48.4	30.48%	2.13%	0.10%
50 t/ha	Carbonation	63.2	39.79%	2.77%	0.14%
	EW	121	76.19%	5.31%	0.26%

Mt = 10^9 kg

stage, transport and application of dust products may have adverse health effects for practitioners (Schenker et al., 2009; Taylor et al., 2016). In addition, fine grinding or milling demands major energy input (Orumwense and Forssberg, 1992) that could offset the potential sequestration of EW or carbonation. The case for further milling of the <5 mm fraction typically produced in construction aggregate crushing operations would need to be supported by evidence of the associated costs and benefits.

According to the "catchment scale-based conversion" used in Strefler et al. (2018) to estimate the share of spread material that weathered within one year (depending on grain size), the application of 5 mm basalt particles on soil at pH 7 and 25 °C would result in the dissolution of 0.021% of the material after one year. However, this calculation is theoretical and idealized for it ignores the shrinking of the particles as they weather, and the particle size distribution (the <5 mm fraction is a size range). Moreover, none of the factors such as the climatic condition, soil type, presence of vegetation, microorganisms, and fungi, and concentration of atmospheric CO_2 (all known to affect the weathering rate of silicate rocks) are taken into account (Beaulieu et al., 2010; Harley and Gilkes, 2000; Kantola et al., 2017; Li et al., 2016; Manning, 2018; Manning and Renforth, 2013; Moosdorf et al., 2014; Opolot and Finke, 2015; Strefler et al., 2018).

In addition, as the grain size of a final construction aggregate product gets smaller, the co-production of quarry fines (material <5 mm) increases. Although their production depends on various factors (e.g. mineral composition and texture of the rock, crusher type and number of stages) the production of 10 mm aggregate usually result in 35–40% of fines <5 mm by weight (Mitchell et al., 2008). A product with low amounts of use in the aggregate industry, these fines could be spread on the field for EW or carbonation where they will rapidly weather (Manning et al., 2013).

Precisely predicting the weathering rates without measurements from local field experiments is, as yet, impossible because of the manifold parameters involved. However, the tropical climate, acidic soils, and the presence of vegetation on the application area considered in our study as well as the substantial proportion of material <5 mm should ensure a faster weathering rate than the 0.021% per year calculated here above.

Weathering rate, along with the vertical transportation of the applied material through soil by percolation and bioturbation (disturbance of soil by living organisms) (Taylor et al., 2016), are crucial for they determine the delay between applications. This delay is essential to maintain the balance of the amended site and ensure durability of the potential benefits associated with the technique. As neither of those parameters were precisely considered in this study, the sequestered amount presented should not be considered as annual.

4.4. Maximum travel distance to offset potential capture

Basalt extraction, crushing and spreading induce fixed emissions (discussed in Section 3.1). However, as the quarry to field distance increases, the emissions associated with transport further reduce the sequestration potential of the practice. Based on the linear relationship between delivery distance and transport GHG emissions, the distance at which the carbon capture potential of basalt application is completely offset is about 540 and 990 km of road travel for carbonation and EW respectively. This distance is independent of the amount of basalt processed, as the emissions associated with the processes increase proportionally with the potential sequestration through carbonation and EW. These offsetting distances are proportionally related to the potential sequestration of each path due to the linear increase of GHG emissions and distance as discussed before.

In a global assessment, Moosdorf et al. (2014) suggest that "*The transportation CO_2 emissions from source to application areas average 0.007 (0.022) t CO_2 t^{-1}* [optimistic (pessimistic) scenarios; t^{-1}: per tonne of rock]" considering transportation by railroad, road and waterways. From our hypothetical system and the average quarry

to field distance of 65 km, we reach an average emission of 0.011 t CO_{2eq} per tonne of rock, which is within the range of Moosdorf et al. (2014). Yet, our hypothetical system is located on part of a large flood basalt outcrop where spatial density of basalt quarries can be assumed higher than in other parts of the world. The underestimation of transportation impact is seen further where Moosdorf et al. (2014) state that the maximum distance (at which the emission offset the capture potential) is 17,000 (5000) km by road when considering a potential sequestration of 1.1 (0.8) tCO_{2eq}/t of rock (optimistic (pessimistic) scenario). Compared with our hypothetical system, Moosdorf et al. (2014)'s optimistic and pessimistic predictions are overestimated by 72 and 30%, respectively. This difference is due to the fact that Moosdorf et al. (2014) considered global routes from source rock location to each continuous area of arable land.

Considering other means of transportation, such a railroad or inland waterways, the offsetting distance is increased. According to SimaPro 8.3.0, the waterway and railroad processes emit around 3.5 times less CO_2/tkm than the truck considered for road transport.

Assuming that 50 km of road transportation is necessary from the quarry to the station/harbour and another 50 km is necessary to reach the field after railroad/waterway transportation, the offsetting distance considering carbonation would reach around 2200 and 2140 km through railroad and waterway, respectively. Regarding EW, these distances increase to around 4300 and 4200 km through railroad and waterway, respectively.

4.4.1. Impact of uncertainties on offsetting distance

Our uncertainty analysis (in the supplementary material) showed that the most uncertain parameters in our assessment are i) the fraction of the cations that will be transferred to the ocean (ω value); and ii) the type of truck used to set up the practice (emission factor). In Fig. 8, we show the impacts of both these parameters on the offsetting distance of the practice. The error bars on the figure represent the propagation of the uncertainty associated with all the other processes. Based on our uncertainty analysis, the error in the ω value represents around 11% of the mean sequestration potential and errors in the different process stages represent around 5% of the emissions.

Fig. 8 highlights the influence of the emission factor (in $kgCO_{2eq}$/tkm) of the truck selected for the transportation of the material (threefold difference between most and least efficient trucks) as well as the impact of the additional sequestration due to the transfer of the cations to the ocean (ω value) on the offsetting distance. Hauliers would usually use the largest vehicle possible, given the road conditions.

4.5. Comminution and energy requirement

Based on the conversion factor of SimaPro 8.3 from Brazilian electricity to $kgCO_{2eq}$ we calculated the energy required to offset the sequestration values, considering the average quarry to field distance of 65 km. The energy needed to offset the sequestration potential of the practices is around 276 and 529 kWh for carbonation and EW, respectively.

Therefore, considering Bond's equation, the energy required to reach 5 mm particles, the additional equipment needed to consider the grinding facility, and the emissions associated with the other process stages (average quarry to field distance of 65 km), the particle size to reach this offsetting energy demand would be

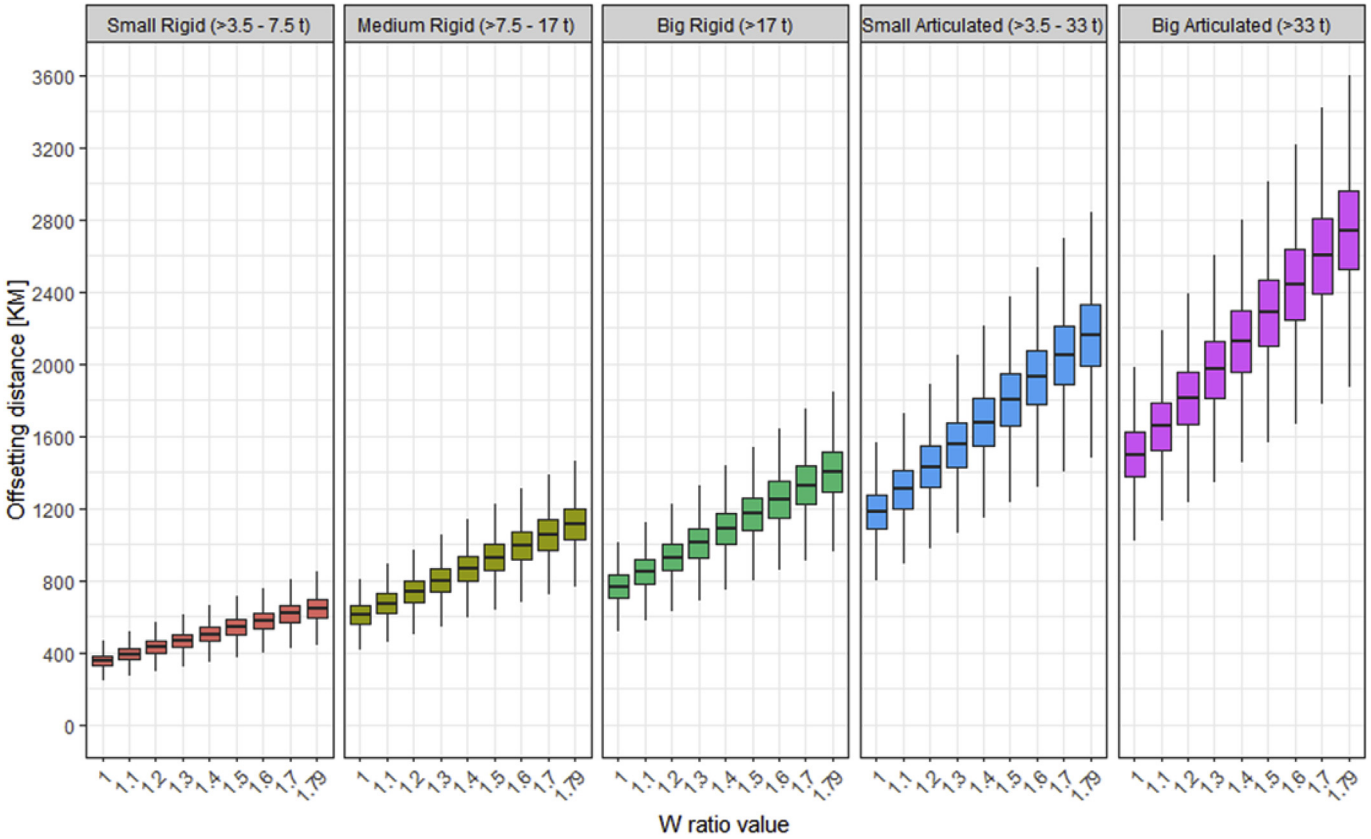

Fig. 8. Effect of Emission Factor (truck type) and W value on the offsetting distance. The W value of 1 and 1.79 represent Carbonation and EW, respectively. The error bars represent the propagation of the uncertainty on emissions associated with all the other processes as well as the uncertainty on sequestration potential according to the W value.

0.00062 mm and 0.00032 mm for carbonation and EW, respectively. Although further comminution induces a steep increase of energy, the particle size to offset the sequestration potential is, in practice, unreachable.

The distance at which the setup of the practice offsets the sequestration potential is based on the emissions associated with the implementation of the practice. As the particle size decreases, the emissions increase and so reduce the offsetting distance of the practice. When the final particle size is 5 mm, the offsetting distances are 544 and 994 km by road for carbonation and EW, respectively. When the final particle size reaches 0.02 mm the offsetting distances decline to 526 and 977 km for carbonation and EW, respectively. The distance decreases exponentially with lower particle size due to the exponential increase in energy requirement as the product particle size decreases.

4.6. Basalt production in SP and relevance of the proposed application rate

According to the data extracted from UCLouvain (2017), Sao Paulo state has a total of 11.7 million hectares of cropland and grassland.

Therefore, 58.5, 234, and 585 million tonnes of basalt would be needed to amend the land considering our three application rates of 5, 20, and 50 tonnes per hectare, respectively.

The representative quarry used in this study has an annual production of 450,000 tonnes (Rosado et al., 2017) and is considered as a medium size facility (DNPM, 2018). To reach the application rates of 5, 20, and 50 t/ha proposed annually, Sao Paulo state would need 130, 520, 1300 medium size facilities producing 450,000 t/year, respectively. However, according to DNPM (2018), Sao Paulo state had a total of 47 basalt quarries in 2015: 1 big facility (>1,000,000 t/year), 32 medium size ([100,000–1,000,000] t/year), 13 small ([10,000–100,000] t/year) and 1 micro facility (<10,000 t/year).

If we consider an average production of 450,000 t/year for each facility, and the allocation of 100% of the production to the practice, the conceivable application rate reaches 1.8 t/ha.

Despite being strongly approximated, these numbers shed light on the mismatch of the application rate sometimes considered in publications. As shown above, transport distances play a key role in the sequestration potential of the practice. Considering an application rate of 50 t/ha while staying in the geographical range of already existing basalt quarries overshoots their production capacity, which would need to increase by a factor of 3 (5 t/ha) −10 (20 t/ha) to have a reasonable impact. This could be achieved either by expanding existing quarries or by creating new quarries.

5. Conclusion

In this study, we have shown that an existing network of basalt quarries, already producing construction aggregates at low cost, has the potential to supply a region with crushed material suitable for enhanced weathering or carbonation. Our LCA distinguished fixed and transport-related burdens of extraction, delivery and application, and enabled us to assess the net CO_2 sequestration benefit from using ground basalt on agricultural soil.

We showed that transportation of the ground material greatly affects the potential sequestration of the technique. In our case study, the maximum delivery distances before basalt management emissions exceeded CO_2 sequestration were 544 ± 65 and 994 ± 116 km when considering carbonation and EW, respectively. Comparisons with previously published assessment show logistics and transport impacts can be underestimated, leading to over-optimistic sequestration values.

Considering Sao Paulo state sequestration potential, our study shows that the application of crushed basalt could capture 1.3 to 2.4 Mt CO_{2eq} through the application rate of 1 t/ha applied on all its 12 million hectares through carbonation and enhanced weathering respectively, including the emissions associated with the setup of the practice.

We considered the likely positive soil and crop response to basalt addition that could increase the sequestration potential of the practice as well as potential negative effects that warrant further experimental investigation.

Finally, as various techniques are increasingly promoted as efficient solutions to remove or sequester CO_2, this study emphasizes the need to consider the practice in its entirety to show the limitations and potential caveats. The holistic approach of LCA helps in identifying the processes with the largest impacts and their significance. However, its precision and reliability are only as high as the amount, quality and representability of the input data. Therefore, fundamental studies on each process stage considered should be conducted, focusing on local practices to increase accuracy.

Declarations of interest

None.

Acknowledgments

We acknowledge funding through the UP-Green-LCA (NE/P019668/1) and SOILS-R-GGREAT (NE/P019498/1) projects of the greenhouse gas removal (GGR) programme. The GGR programme is financed by the UK Natural Environment Research Council (NERC), Engineering and Physical Sciences Research Council, Economic and Social Science Research Council (ESRC) and the UK department for Business, Energy and Industrial Strategy (BEIS). The authors wish to acknowledge the Royal Society for providing precious insights at the Sackler Forum in 2017. No new data were collected in the course of this research. This study was an analysis of existing data that are publicly available from the cited literature.

Appendix A. Supplementary data

Supplementary data to this article can be found online at https://doi.org/10.1016/j.jclepro.2019.06.099.

References

Araújo, M. da P.S., Campos, V.B.G., Bandeira, R.A.M., 2013. An overview of road cargo transport in Brazil. Int. J. Ind. Eng. Manag. URL [WWW Document]. http://ijiemjournal.org/images/journal/volume4/ijiem_vol4_no3_7.pdf.

Baggio, S.B., Hartmann, L.A., Bello, R.M.S., 2016. Paralavas in the cretaceous paraná volcanic province, Brazil - a genetic interpretation of the volcanic rocks containing phenocrysts and glass. An. Acad. Bras. Cienc. 88, 2167–2193. https://doi.org/10.1590/0001-3765201620150088.

Beaulieu, E., Goddéris, Y., Labat, D., Roelandt, C., Oliva, P., Guerrero, B., 2010. Impact of atmospheric CO2 levels on continental silicate weathering. Geochem. Geophys. Geosyst. 11. https://doi.org/10.1029/2010GC003078.

Beerling, D.J., 2017. Enhanced rock weathering: biological climate change mitigation with co-benefits for food security? Biol. Lett. 13, 4–7. https://doi.org/10.1098/rsbl.2017.0149.

Beerling, D.J., Leake, J.R., Long, S.P., Scholes, J.D., Ton, J., Nelson, P.N., Bird, M.I., Kantzas, E., Taylor, L.L., Sarkar, B., Kelland, M., DeLucia, E., Kantola, I., Müller, C., Rau, G.H., Hansen, J., 2018. Farming with crops and rocks to address global climate, food and soil security. Nat. Plants 4, 138–147. https://doi.org/10.1038/s41477-018-0108-y.

Bergmann, M., Silveira, C.A.P., Bandeira, R., Bamberg, A., Martinazzo, R., Grecco, M., 2013. Amygdaloidal basalts to zeolites of the "serra geral" formation of Paraná Basin : potential agronomic use [WWW Document]. Brazilian Stonemeal Conf. URL. https://remineralize.org.

Berner, R.A., Kothavala, Z., 2001. GEOCARB III; a revised model of atmospheric CO2 over phanerozoic time. Am. J. Sci. 301, 182–204. https://doi.org/10.2475/ajs.294.

1.56.
Braz Machado, F., Reis, E., Rocha-Júnior, V., Soares Marques, L., José, A., Nardy, R., Vieira Zezzo, L., Marteleto, N.S., 2018. Geochemistry of the northern paraná continental flood basalt (PCFB) province: implications for regional chemostratigraphy. Brazilian J. Geol. 48, 177–199. https://doi.org/10.1371/journal.pone.0018728.
Bryan, S.E., Ernst, R.E., 2008. Revised definition of large igneous provinces (LIPs). Earth-Science Rev. 86, 175–202. https://doi.org/10.1016/j.earscirev.2007.08.008.
Campe, J., Kittredge, D., Klinger, L., 2015. The Potential of Remineralization with Rock Mineral Fines to Transform Agriculture, Forests, Sustainable Biofuels Production, Sequester Carbon, and Stabilize the Climate [WWW Document]. URL. http://remineralize.org/wp-content/uploads/2015/10/ODB1.pdf.
CNT Confederacao National do Transporte, 2017. Pesquisa de Rodovias Sudeste [MAP]. WWW Document]. URL. http://pesquisarodovias.cnt.org.br/Paginas/mapa-por-regiao-uf.
Core Team, R., 2018. R: A Language and Environment for Statistical Computing. R Foundation for Statistical Computing. WWW Document]. URL. https://www.r-project.org/.
DNPM, 2018. Cadastro nacional de Produtores de Brita - ano base 2015. WWW Document]. URL. http://www.dnpm.gov.br.
EASAC, 2018. Negative emission technologies: what role in meeting Paris Agreement targets? [WWW Document]. URL. https://easac.eu.
Edwards, D.P., Lim, F., James, R.H., Pearce, C.R., Scholes, J., Freckleton, R.P., Beerling, D.J., Edwards, D.P., 2017. Climate change mitigation : potential benefits and pitfalls of enhanced rock weathering in tropical agriculture. Biol. Lett. https://doi.org/10.1098/rsbl.2016.0715.
ESRI, 2011. ArcGIS desktop. WWW Document]. URL. http://desktop.arcgis.com.
Fantke, P., Bijster, M., Guignard, C., Hauschild, M., Huijbregts, M., Jolliet, O., Kounina, A., Magaud, V., Margni, M., McKone, T., Posthuma, L., Rosenbaum, R.K., van de Meent, D., van Zelm, R., 2017. USEtox® 2.0, Documentation (Version 1), (Ed.) https://doi.org/10.11581/DTU:00000011.
Felipe, F.I., Lima, R.A.D.S., Rodrigues, S.M., 2008. Evolução da estrutura da indústria de tratores de rodas, no Brasil, no período de 1999 a 2008. https://www.cepea.esalq.usp.br.
Frischknecht, R., N.J., Althaus, H., Bauer, C., Doka, G., Dones, R., Hischier, R., Hellweg, S., Köllner, T., Loerincik, Y., Margni, M., 2007. Implementation of Life Cycle Impact Assessment Methods. In: Editors (Ed.). WWW Document]. Am. Midl. Nat. URL. http://www.ecoinvent.org/fileadmin/documents/en/03_LCIA-Implementation.pdf.
Fuss, S., Canadell, J.G., Peters, G.P., Tavoni, M., Andrew, R.M., Ciais, P., Jackson, R.B., Jones, C.D., Kraxner, F., Nakicenovic, N., Le Quéré, C., Raupach, M.R., Sharifi, A., Smith, P., Yamagata, Y., 2014. Betting on negative emissions. Nat. Clim. Chang. 4, 850–853. https://doi.org/10.1038/nclimate2392.
Fuss, S., Lamb, W.F., Max, W., Nemet, G.F., Callaghan, M.W., Stechow, C. Von, Minx, J.C., Fuss, S., Lamb, W.F., Callaghan, M.W., Beringer, T., Garcia, W.D.O., Hartmann, J., Khanna, T., Minx, J.C., 2018. Negative emissions — Part 2: costs , potentials and side effects. Environ. Res. Lett. 13, 063002. https://doi.org/10.1088/1748-9326/aabf9f.
Gillman, G.P., Burkett, D.C., Coventry, R.J., 2002. Amending highly weathered soils with finely ground basalt rock. Appl. Geochem. 17, 987–1001. https://doi.org/10.1016/S0883-2927(02)00078-1.
Goglio, P., Smith, W.N., Worth, D.E., Grant, B.B., Desjardins, R.L., Chen, W., Tenuta, M., McConkey, B.G., Williams, A., Burgess, P.J., 2018. Development of Crop.LCA, an adaptable screening life cycle assessment tool for agricultural systems: a Canadian scenario assessment. J. Clean. Prod. 172, 3770–3780. https://doi.org/10.1016/j.jclepro.2017.06.175.
Goldich, S.S., 1938. A study in rock-weathering. J. Geol. 46, 17–58. https://doi.org/10.1086/624619.
Golsteijn, Laura, 2014. How to use USEtox® characterisation factors in SimaPro | PRé sustainability [WWW Document]. URL. https://www.pre-sustainability.com/news/how-to-use-usetox-characterisation-factors-in-simapro. accessed,10,16,2018.
Google, 2018. Google Earth pro. WWW Document]. URL. https://www.google.com/earth/download/gep/agree.html.
Guinee, J.B., Gorree, M., Heijungs, R., Huppes, G., Kleijn, R., van Oers, L., Sleeswijk, A.W., Suh, S., Udo de Haes, H.A., de Bruijn, H., van Duin, R., Huijbregts, M.A.J., 2002. Handbook on Life Cycle Assessment, Operational Guide to the ISO Standards, Eco-Efficiency in Industry and Science. Springer Netherlands, Dordrecht. https://doi.org/10.1007/0-306-48055-7.
Harley, A.D., Gilkes, R.J., 2000. Factors influencing the release of plant nutrient elements from silicate rock powders: a geochemical overview. Nutr. Cycl. Agroecosyst. 56, 11–36. https://doi.org/10.1023/A:1009859309453.
Hartmann, J., Moosdorf, N., 2012. The new global lithological map database GLiM: a representation of rock properties at the Earth surface. Geochem. Geophys. Geosyst. 13, 1–37. https://doi.org/10.1029/2012GC004370.
Hartmann, J., Jansen, N., Dürr, H.H., Kempe, S., Köhler, P., 2009. Global CO2-consumption by chemical weathering: what is the contribution of highly active weathering regions? Glob. Planet. Chang. 69, 185–194. https://doi.org/10.1016/j.gloplacha.2009.07.007.
Harvey, L.D.D., 2008. Mitigating the atmospheric CO2 increase and ocean acidification by adding limestone powder to upwelling regions. J. Geophys. Res. Ocean. 113, 1–21. https://doi.org/10.1029/2007JC004373.
IBGE, 2017. Resultados do censo agro 2017. WWW Document]. Censo Agro 2017 . URL. https://censoagro2017.ibge.gov.br/templates/censo_agro/resultadosagro/estabelecimentos.html?localidade=35. (Accessed 9 November 2018).
IPCC, 2014. Climate Change 2013: the Physical Science Basis, Contribution of Working Group I to the Fifth Assessment Report of the Intergovernmental Panel on Climate Change. Cambridge Univesity Press, Cambridge, United Kingdom and New York, NY, USA.
Kanda, Y., Kotake, N., 2007. Comminution energy and evaluation in fine grinding, in: handbook of powder technology. https://doi.org/10.1016/S0167-3785(07)12015-7, 529 550.
Kantola, I.B., Masters, M.D., Beerling, D.J., Long, S.P., Delucia, E.H., 2017. Potential of global croplands and bioenergy crops for climate change mitigation through deployment for enhanced weathering. Biol. Lett. https://doi.org/10.1098/rsbl.2016.0714.
Kheshgi, H.S., 1995. Sequestering atmospheric carbon dioxide by increasing ocean alkalinity. Energy 20, 915–922. https://doi.org/10.1016/0360-5442(95)00035-6.
Khoo, H.H., Bu, J., Wong, R.L., Kuan, S.Y., Sharratt, P.N., 2011. Carbon capture and utilization: preliminary life cycle CO2, energy, and cost results of potential mineral carbonation. Energy Procedia 4, 2494–2501. https://doi.org/10.1016/j.egypro.2011.02.145.
Kohler, P., Hartmann, J., Wolf-Gladrow, D.A., 2010. Geoengineering potential of artificially enhanced silicate weathering of olivine. Proc. Natl. Acad. Sci. 107, 20228–20233. https://doi.org/10.1073/pnas.1000545107.
Kolosz, B.W., Sohi, S. p., Manning, D.A.C., 2019. CASPER: a modelling framework to link mineral carbonation with the turnover of organic matter in soil. Comput. Geosci. 124, 58–71. https://doi.org/10.1016/j.cageo.2018.12.012.
Landi, A., Mermut, A.R., Anderson, D.W., 2003. Origin and rate of pedogenic carbonate accumulation in Saskatchewan soils, Canada. Geoderma 117, 143–156. https://doi.org/10.1016/S0016-7061(03)00161-7.
Leonardos, O.H., Theodoro, S.H., Assad, M.L., 1998. Remineralization for sustainable agriculture: a tropical perspective from a Brazilian viewpoint. Nutr. Cycl. Agroecosyst. 56, 3–9. https://doi.org/10.1023/A:1009855409700.
Li, G.G., Hartmann, J., Derry, L.A., West, A.J., You, C.F., Long, X., Zhan, T., Li, L., Li, G.G., Qiu, W., Li, T., Liu, L., Chen, Y., Ji, J., Zhao, L., Chen, J., 2016. Temperature dependence of basalt weathering. Earth Planet. Sci. Lett. 443, 59–69. https://doi.org/10.1016/j.epsl.2016.03.015.
Manfré, L.A., de Albuquerque Nóbrega, R.A., Quintanilha, J.A., 2015. Regional and local topography subdivision and landform mapping using SRTM-derived data: a case study in southeastern Brazil. Environ. Earth Sci. 73, 6457–6475. https://doi.org/10.1007/s12665-014-3869-2.
Manning, D.A.C., 2010. Mineral sources of potassium for plant nutrition. A review. Agron. Sustain. Dev. 30, 281–294. https://doi.org/10.1051/agro/2009023.
Manning, D.A.C., 2018. Innovation in resourcing geological materials as crop nutrients. Nat. Resour. Res. 27, 217–227. https://doi.org/10.1007/s11053-017-9347-2.
Manning, D.A.C., Renforth, P., 2013. Passive sequestration of atmospheric CO2 through coupled plant-mineral reactions in urban soils. Environ. Sci. Technol. 47, 135–141. https://doi.org/10.1021/es301250j.
Manning, D.A.C., Renforth, P., Lopez-Capel, E., Robertson, S., Ghazireh, N., 2013. Carbonate precipitation in artificial soils produced from basaltic quarry fines and composts: an opportunity for passive carbon sequestration. Int. J. Greenh. Gas Control 17, 309–317. https://doi.org/10.1016/j.ijggc.2013.05.012.
Martin, J.B., 2017. Carbonate minerals in the global carbon cycle. Chem. Geol. 449, 58–72. https://doi.org/10.1016/j.chemgeo.2016.11.029.
Massey, F.P., Roland Ennos, A., Hartley, S.E., 2007. Herbivore specific induction of silica-based plant defences. Oecologia 152, 677–683. https://doi.org/10.1007/s00442-007-0703-5.
Melo, V.F., Uchôa, S.C.P., Dias, F. de O., Barbosa, G.F., 2012. Doses de basalto moído nas propriedades químicas de um Latossolo Amarelo distrófico da savana de Roraima. Acta Amaz 42, 471–476. https://doi.org/10.1590/S0044-59672012000400004.
Mersi, W. Von, Kuhnert-Finkernagel, R., Schinner, F., 1991. The influence of rock powders on microbial activity of three forest soils. Zeitschrift für Pflanzenernährung und Bodenkd. 155, 29–33. https://doi.org/10.1002/jpln.19921550107.
Metso, 2015. Basics in minerals processing. WWW Document]. URL. https://www.metso.com.
Meysman, F.J.R., Montserrat, F., 2017. Negative CO2 emissions via enhanced silicate weathering in coastal environments. Biol. Lett. 13, 20160905. https://doi.org/10.1098/rsbl.2016.0905.
Mitchell, C., Mitchell, P., Pascoe, R., 2008. Quarry fines minimisation: can we really have 10mm aggregate with no fines? [WWW Document]. Walton, Geoffrey, Proc. 14th Extr. Ind. Geol. Conf. URL http://nora.nerc.ac.uk/4854/.
Moosdorf, N., Renforth, P., Hartmann, J., 2014. Carbon dioxide efficiency of terrestrial enhanced weathering. Environ. Sci. Technol. 48, 4809–4816. https://doi.org/10.1021/es4052022.
Moraes, L.C. de, Seer, H.J., Marques, L.S., 2018. Geology, geochemistry and petrology of basalts from paraná continental magmatic province in the araguari, uberlândia, uberaba and sacramento regions, minas gerais state, Brazil. Brazilian J. Geol. 48, 221–241. https://doi.org/10.1590/2317-4889201820170091.
Nduagu, E., Bergerson, J., Zevenhoven, R., 2012. Life cycle assessment of CO2 sequestration in magnesium silicate rock - a comparative study. Energy Convers. Manag. 55, 116–126. https://doi.org/10.1016/j.enconman.2011.10.026.
Nunes, J.M.G., Kautzmann, R.M., Oliveira, C., 2014. Evaluation of the natural fertilizing potential of basalt dust wastes from the mining district of Nova Prata (Brazil). J. Clean. Prod. 84, 649–656. https://doi.org/10.1016/j.jclepro.2014.04.032.
Olivier, J.G.J., Schure, K.M., Peters, J.A.H.W., 2017. Trends in Global CO2 and Total

Greenhouse Gas Emissions [WWW Document]. PBL Netherlands Environ. Assess. Agency. http://www.pbl.nl.
Opolot, E., Finke, P.A., 2015. Evaluating sensitivity of silicate mineral dissolution rates to physical weathering using a soil evolution model (SoilGen2.25). Biogeosciences 12, 6791–6808. https://doi.org/10.5194/bg-12-6791-2015.
Orumwense, O.A., Forssberg, E., 1992. Superfine and ultrafine grinding - a literature. Survey. Miner. Process. Extr. Metall. Rev. An Int. J. 11, 107–127. https://doi.org/10.1080/08827509208914216.
O'Connor, W.K., Dahlin, D.C., Rush, G.E., Gerdemann, S.J., Penner, L.R., Nilsen, D.N., 2005. Aqueous Mineral Carbonation: Mineral Availability, Pretreatment, Reaction Parametrics, and Process Studies. DOE. https://doi.org/10.13140/RG.2.2.23658.31684.
Perrotta, M.M., Salvador, E.D., Lopes, R. da C., D'agostino, L.Z., Chieregati, L.A., Peruffo, N., Gomes, S.D., Sachs, L.L.B., Meira, V.T., Garcia, M., da, G.M., Larceda Filho, J.V. de, 2006. Geologia e recursos minerais do estado de São Paulo. WWW Document]. URL. http://rigeo.cprm.gov.br/jspui/handle/doc/2966. accessed 8.15.18.
Ramezanian, A., Dahlin, A.S., Campbell, C.D., Hillier, S., Mannerstedt-Fogelfors, B., Öborn, I., 2013. Addition of a volcanic rockdust to soils has no observable effects on plant yield and nutrient status or on soil microbial activity. Plant Soil 367, 419–436. https://doi.org/10.1007/s11104-012-1474-2.
Ramos, C.G., Querol, X., Oliveira, M.L.S., Pires, K., Kautzmann, R.M., Silva, L.F.O., 2015. A preliminary evaluation of volcanic rock powder for application in agriculture as soil a remineralizer. Sci. Total Environ. 512–513, 371–380. https://doi.org/10.1016/j.scitotenv.2014.12.070.
Ramos, C.G., Querol, X., Dalmora, A.C., de Jesus Pires, K.C., Schneider, I.A.H., Silva, L.F.O., Kautzmann, R.M., 2017. Evaluation of the potential of volcanic rock waste from southern Brazil as a natural soil fertilizer. J. Clean. Prod. 142, 2700–2706. https://doi.org/10.1016/j.jclepro.2016.11.006.
REMIN, n.d Improve Soil Health with Rock Dust | REMIN Scotland Ltd [WWW Document]. URL http://www.reminscotland.com/home/how-to-use/(accessed 9.21.2018).
Renforth, P., 2012. The potential of enhanced weathering in the UK. Int. J. Greenh. Gas Control 10, 229–243. https://doi.org/10.1016/j.ijggc.2012.06.011.
Renforth, P., Washbourne, C.L., Taylder, J., Manning, D.A.C., 2011. Silicate production and availability for mineral carbonation. Environ. Sci. Technol. 45, 2035–2041. https://doi.org/10.1021/es103241w.
Renforth, P., Pogge von Strandmann, P.A.E., Henderson, G.M., 2015. The dissolution of olivine added to soil: implications for enhanced weathering. Appl. Geochem. 61, 109–118. https://doi.org/10.1016/j.apgeochem.2015.05.016.
Rosado, L.P., Vitale, P., Penteado, C.S.G., Arena, U., 2017. Life cycle assessment of natural and mixed recycled aggregate production in Brazil. J. Clean. Prod. 151, 634–642. https://doi.org/10.1016/j.jclepro.2017.03.068.
Schenker, M.B., Pinkerton, K.E., Mitchell, D., Vallyathan, V., Elvine-Kreis, B., Green, F.H.Y., 2009. Pneumoconiosis from agricultural dust exposure among young California farmworkers. Environ. Health Perspect. 117, 988–994. https://doi.org/10.1289/ehp.0800144.
SEEG, 2016a. São Paulo - Emissions [WWW Document]. Syst. Greenh. Gas Emiss. Remov. Estim. http://plataforma.seeg.eco.br/territories/sao-paulo/card?year=2016 (accessed 9.14.18).
SEEG, 2016b. Total Emissions - Brazil [WWW Document]. Syst. Greenh. Gas Emiss. Remov. Estim. http://plataforma.seeg.eco.br/total_emission (accessed 9.14.18).
Smith, P., Davis, S.J., Creutzig, F., Fuss, S., Minx, J., Gabrielle, B., Kato, E., Jackson, R.B., Cowie, A., Kriegler, E., Van Vuuren, D.P., Rogelj, J., Ciais, P., Milne, J., Canadell, J.G., McCollum, D., Peters, G., Andrew, R., Krey, V., Shrestha, G., Friedlingstein, P., Gasser, T., Grübler, A., Heidug, W.K., Jonas, M., Jones, C.D., Kraxner, F., Littleton, E., Lowe, J., Moreira, J.R., Nakicenovic, N., Obersteiner, M., Patwardhan, A., Rogner, M., Rubin, E., Sharifi, A., Torvanger, A., Yamagata, Y., Edmonds, J., Yongsung, C., 2016. Biophysical and economic limits to negative CO2emissions. Nat. Clim. Chang. 6, 42–50. https://doi.org/10.1038/nclimate2870.
Strefler, J., Amann, T., Bauer, N., Kriegler, E., Hartmann, J., 2018. Potential and costs of carbon dioxide removal by enhanced weathering of rocks. Environ. Res. Lett. 13, 034010. https://doi.org/10.1088/1748-9326/aaa9c4.
Taylor, L.L., Quirk, J., Thorley, R.M.S., Kharecha, P.A., Hansen, J., Ridgwell, A., Lomas, M.R., Banwart, S.A., Beerling, D.J., 2016. Enhanced weathering strategies for stabilizing climate and averting ocean acidification. Nat. Clim. Chang. 6, 402–406. https://doi.org/10.1038/nclimate2882.
Taylor, L.L., Beerling, D.J., Quegan, S., Banwart, S.A., 2017. Simulating carbon capture by enhanced weathering with croplands: an overview of key processes highlighting areas of future model development. Biol. Lett. 13. https://doi.org/10.1098/rsbl.2016.0868.
ten Berge, H.F.M., van der Meer, H.G., Steenhuizen, J.W., Goedhart, P.W., Knops, P., Verhagen, J., 2012. Olivine weathering in soil, and its effects on growth and nutrient uptake in ryegrass (Lolium perenne L.): a pot experiment. PLoS One 7. https://doi.org/10.1371/journal.pone.0042098.
Theodoro, S.H., Leonardos, O.H., 2006. The use of rocks to improve family agriculture in Brazil. An. Acad. Bras. Cienc. 78, 721–730. https://doi.org/10.1590/S0001-37652006000400008.
UCLouvain, 2017. Climate Research Data Package (CRDP) [WWW Document]. ESA Clim. Chang. Initiat. URL. http://maps.elie.ucl.ac.be/CCI/viewer/download.php. accessed 8.23.2018.
Wanke, P., Fleury, P.F., 2006. Transporte de cargas no Brasil: estudo exploratório das principais variáveis relacionadas aos diferentes modais e às suas estruturas de custos [WWW Document]. Estrut. e Dinâmica do Set. Serviços no Bras. URL. https://www.en.ipea.gov.br.
Washbourne, C.L., Lopez-Capel, E., Renforth, P., Ascough, P.L., Manning, D.A.C., 2015. Rapid removal of atmospheric CO_2 by urban soils. Environ. Sci. Technol. 49, 5434–5440. https://doi.org/10.1021/es505476d.
Weidema, B.P., Bauer, C., Hischier, R., Mutel, C., Nemecek, T., Reinhard, J., Vadenbo, C.O., Wernet, G., 2013. Data Quality Guideline for the Ecoinvent Database Version 3. WWW Document]. URL. http://www.ecoinvent.org/database/methodology-of-ecoinvent-3/methodology-of-ecoinvent-3.html.
Williamson, P., 2016. Scrutinize CO2 removal methods. Nature 530, 5–7. https://doi.org/10.1038/530153a.
Williamson, P., Bodle, R., 2016. Update on Climate Geoengineering in Relation to the Convention on Biological Diversity: Potential Impacts and Regulatory Framework [WWW Document]. URL. https://www.cbd.int/doc/publications/cbd-ts-84-en.pdf.